DOI: 10.61782/fa.2023.0040

forum acusticum 2023

ACOUSTO-OPTIC DEVICES IN ADVANCED MICROSCOPY

Peter Saggau[1,2,3*]
[1] Department of Neuroscience, Baylor College of Medicine, Houston TX, USA
[2] Department of Nanophysics, Italian Institute of Technology, Genova, Italy
[3] Department of Applied Physics, University of Barcelona, Barcelona, Spain

ABSTRACT

This review presents several advanced microscope designs employing acousto-optic deflectors (AODs). Here, AODs are used as tunable diffraction gratings to control complex illumination patterns at the Fourier plane of an objective lens. This approach can generate desired illumination patterns at the focal plane of a light microscope.
I will describe a selection of our advanced designs, the 3D Random-Access Multi-Photon Microscope, the Standing-Wave Super-Resolution Microscope, and the Frequency-Encoded Multi-Beam Microscope. All reviewed instruments were designed to overcome the throughput limitations of previously used light microscopes in experimental Neuroscience.
Keywords: *chirped acoustic waves, optical standing-wave pattern, back focal plane pattern, bidirectional light propagation, frequency-shifted multi-beam.*

1. INTRODUCTION

Increasing the spatial and temporal resolution are major goals of advanced light microscopy. In many cases, however, only one of these fundamental properties can be improved, often even at the expense of the other one.
An important application of acousto-optic devices (AODs) are tunable optical diffraction gratings. This allows us to acoustically generate and directly manipulate light distribution at the Fourier plane, thereby controlling the desired illumination patterns at the focal plane of a light microscope.

[*] ***Corresponding author***: *saggaup2@gmail.com.*

2. EXAMPLES OF ACOUSTICALLY CONTROLED ADVANCED MICROSCOPES

2.1 3D Random-Access Multi-Photon Microscope

The most popular application of AODs includes lateral steering of a laser beam. Here, AODs operated in Bragg mode are used to control the angle of the 1st diffraction order, which is proportional to the acoustic frequency, to replace traditional galvanometer-based scan mirrors (*Fig.1, Top*). In a microscope, a pair of such AODs, arranged in orthogonal orientation, can position a focal spot in two dimensions, allowing for traditional 2D scanning (*Fig.1, Bottom*).
The inertia-free beam positioning of AODs provides equal access time of all locations within the focal plane, supporting non-traditional random-access (RA) scanning. In RA mode, beam positing speed is only limited by the time the acoustic wave needs to fill the optical aperture of the AOD. As with all sampling systems, dwell times per sample are determined by the number of photons to be collected per location and the resulting signal-to-noise ratio.

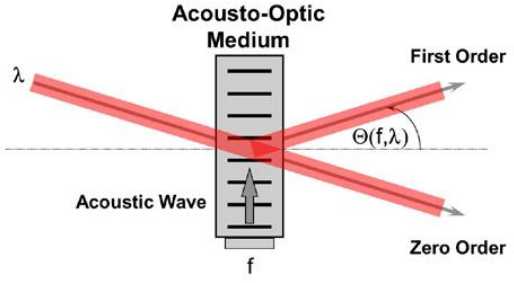

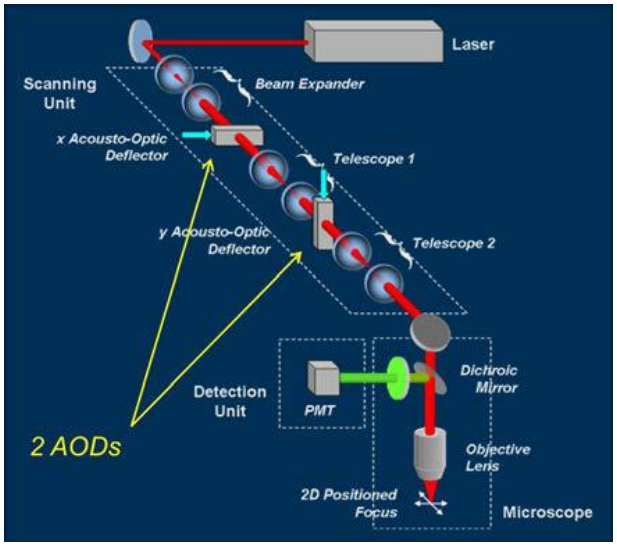

Figure 1. 2D Random-Access Multi-Photon Microscope. *Top:* Bragg-mode AOD. First order beams are commonly used for positioning and scanning applications. *Bottom:* Schematic of 2D RAMP microscope with 2 AODs. Beam conditioning for dispersion compensation not shown.

When using ultrafast lasers for multi-photon excitation of fluorescence, appropriate methods are required to compensate for the strong dispersion of AODs. Two different types of pulse dispersion are observed. To counteract temporal dispersion, a technique named "prechirping" is used to achieve extremely short pulse times in the femto-second range at the specimen. To overcome spatial dispersion, additional diffractive elements are employed to re-collimate diverting beams.

Axial positioning of a focused laser beam in a microscope can be achieved with AODs by utilizing chirped acoustic waves rather than constant frequency waves. Changing the acoustic frequencies faster than their propagation velocity generates a locally varying diffraction grating within the optical aperture (*Fig.2, Top*). This effect can be used to control the collimation of the 1st order beam. Down-chirps result in converging beams, whereas up-chirps produce diverging beams.

When using chirped acoustic waves, besides changes in the collimation, the 1st order beam also undergoes an angular displacement. This effect is unwanted for axial focusing and has to be compensated for. Employing a second AOD with the same chirped acoustic wave propagating in the opposed direction solves this issue. While the changes in collimation add, the angular displacements are compensated (*Fig.2, Bottom*).

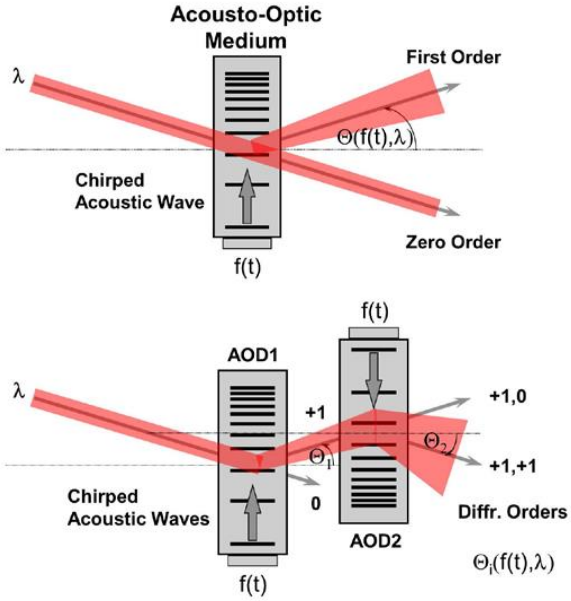

Figure 2. Chirped Acoustic Waves. *Top:* Control of beam collimation by single AOD. Shown is a diverging beam caused by an acoustic down-chirp. *Bottom:* Independent control of collimation and lateral displacement of beam by two AODs with counter-propagating acoustic waves.

Employing two orthogonal pairs of AODs with counter-propagating acoustic waves allows for independently controlling angular displacement and beam collimation, and in consequence any desired combination of lateral and axial positioning at the focal plane of a microscope (*Fig.3, Top*). While the axial position is obtained by a chirp applied to all 4 AODs, the lateral position is due to a frequency offset at only one AOD per pair. As all 4 AODs are addressed at the same time, no time penalty comes with this scheme and the sampling speed in 3D RA mode remains the same.

The high sampling rate of the 3D RAMP microscope supports high-speed monitoring of spiking behavior in a large population of neurons. The total sampling rate of 50 KHz is distributed over the number of monitored cells. For example, 500 cells can be sampled at a rate of 100 volumes per second (*Fig.3, Bottom*).

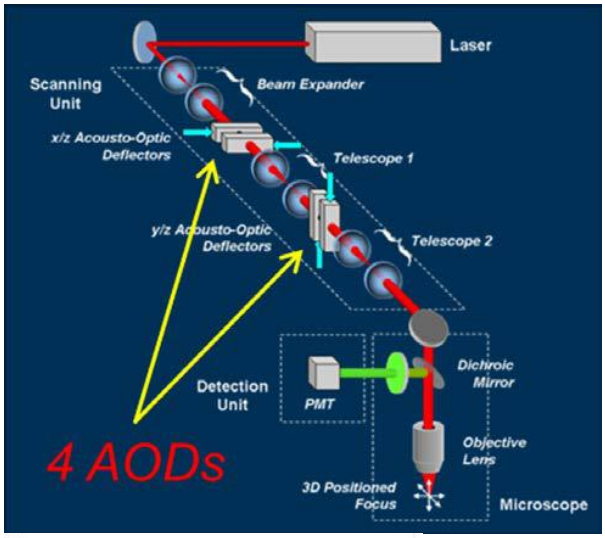

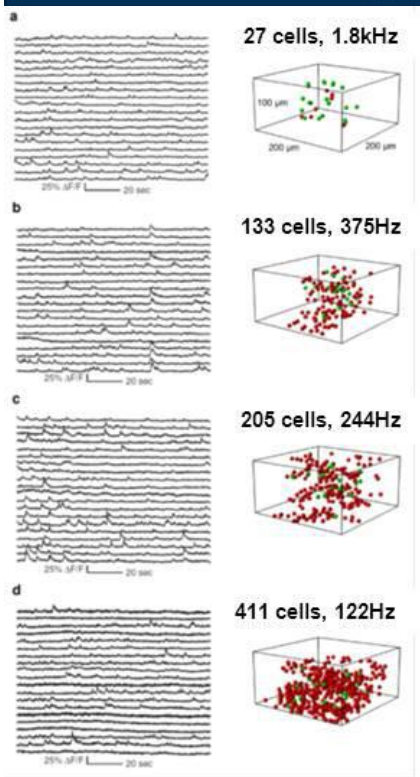

Figure 3. 3D Random-Access Multi-Photon Microscope. *Top:* 3D RAMP microscope with 4 AODs with counter-propagating chirped acoustic waves in 2 pairs of AODs. *Bottom:* Single-cell calcium activity of 20 selected neurons in the mouse visual cortex. Indicated is total number of sampled neurons and corresponding volume sampling rate. Imaged volume 200 µm x 200 µm x 100 µm. Total sampling rate 50 KHz.

Another advantage of using 4-AOD design is the intrinsic compensation of spatial dispersion which occurs with ultrafast laser pulses and does not require the additional diffraction grating needed in the traditional scheme using two AODs. Therefore, the 4 AOD design is well-suited for 3D random-access multi-photon (3D RAMP) microscopes [1, 2].

2.2 Standing-Wave Super-Resolution Microscope

The resolution of an imaging system is determined by its Optical Transfer Function (OTF) and the equivalent Point Spread Function (PSF). Limited PSF and OTF result in loss of high spatial frequencies creating blurred images (*Fig.4, Top*). The intent of super-resolution techniques is to sharpen the PSF and thus widen the OTF passband, as they are Fourier Transforms of each other.

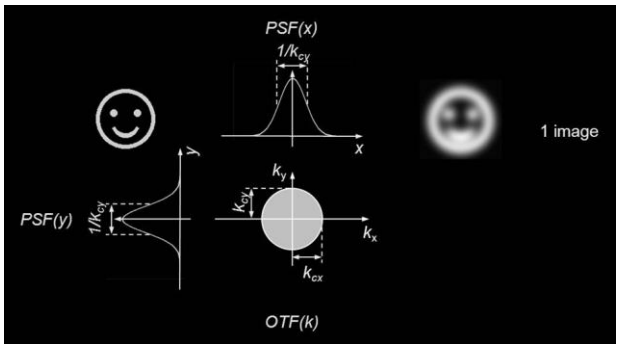

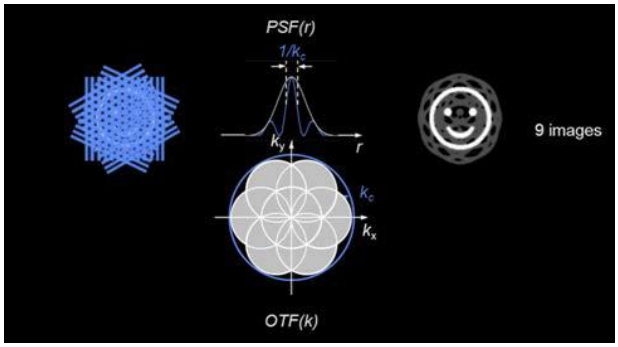

Figure 4. Structured Illumination Principle. *Top:* Loss of high spatial frequencies of image due to limited PSF and OTF. *Bottom:* Structured illumination (SI) improves resolution through sharpened PSF by modulation and extended OTF by additional passband copies. Shown is resolution improvement computed from 9 images obtained with 3 orientations and 3 phases of SI pattern.

Structured Illumination (SI) of the object can increase the resolution of an imaging system. This approach introduces high spatial modulation to the PSF, adding copies of the passband to the OTF, thus allowing higher spatial frequencies to be transmitted. However, this requires capturing multiple images at different orientations and phases of the illumination pattern. An image with improved resolution can then be computed from the acquired set of images (*Fig.4, Bottom*).

One way to create an SI pattern is to generate a Standing Wave (SW) in the focal plane of a microscope. An elegant method to achieve this is by two focal spots at the Back-Focal Plane (BFP) of the objective lens. This will result in two collimated beams at the focal plane which will interfere with the desired SW pattern (*Fig.5, Insets Left & Bottom Center*). An alternative explanation of this scheme is to regard the SI pattern as a cosine intensity modulation. The Fourier transform of the objective lens determines the required BFP illumination – two delta functions – the two focal spots.

The use of AODs allows for an elegant and extremely fast way to generate the required SI pattern (*Fig.5, Top & Right*). In an interferometric scheme, 2 pairs of xy-AODs and a single shared lens form 2 focal spots at the BFP of an objective lens which re-combines the beams. The SW-creating interference happens at the focal plane. In this BFP scanner configuration, the AODs control all parameters of the SI pattern. The separation between the focal spots transforms into the period of the SW, more separation means higher stripe frequency. The orientation of the focal spots on a circle centered at the optical axis gives the direction of the SW. The phase difference of the spots, created by changing the phase of the acoustic wave, moves the SW in radial direction. The inertia-free operation of AODs results in times to change SW pattern of about 10 µs, or less than 100 µs for the full set of 9 patterns. Therefore, the imaging throughput of this SW super-resolution microscope is only limited by the camera speed or the time to collect sufficient photons for a good signal-to-noise ratio.

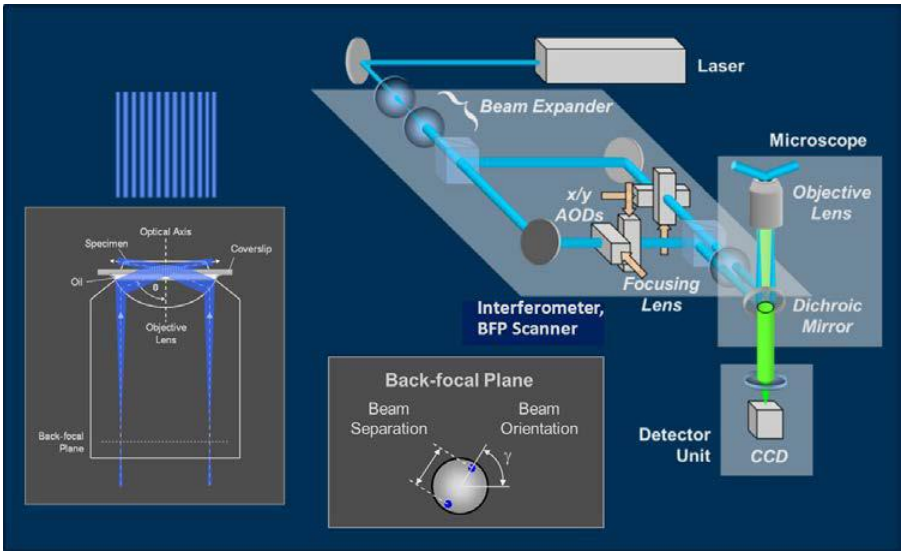

Figure 5. Standing Wave Microscope. *Insets Left & Bottom Center*: Two focal spots at a diagonal of the objective lens BFP create periodic amplitude modulation at sample plane. *Top & Right*: Interferometer containing BFP scanner with 2 pairs of xy-AODs and a shared Focusing Lens to control separation, orientation, and phase of focal spot pair. BFP pattern transforms into period, orientation, and phase of the SW at ample plane. Note: Objective Lens is part of Interferometer.

Resolution improvement was demonstrated by imaging fluorescent beads with a diameter of 100 nm (*Fig.6*). The beads were illuminated at 488 nm and the objective lens specifications were mag = 100x and NA = 1.45. Bead diameters were measured as Full-Width-at-Half-Max (FWHM) of the observed intensity distribution. In Wide-Field Microscopy (WFM) setting, a bead diameter of 270 nm was measured. Deconvolution gave a corrected

diameter of 172 nm. Using our SW Microscope (SWM), a diameter of 109 nm was determined, however, some ghost images remained. Applying the same correction approach, this value was reduced to 101 nm as the Deconvolved SWM diameter. With 50 nm beads the resolution of this SMW was determined to be 80 nm.

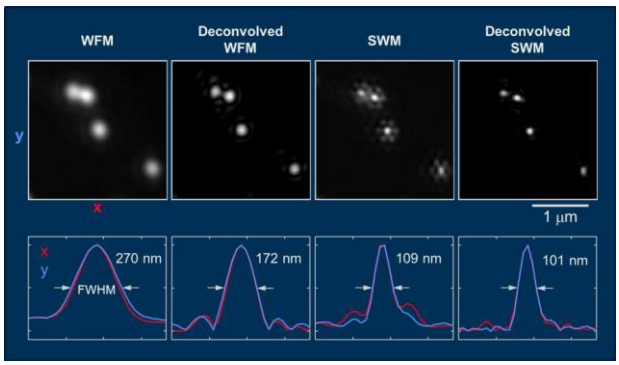

Figure 6. Demonstration of Resolution Improvement., Wide-Field Microscopy (WFM), FWHM = 270 nm, Deconvolved WFM, FWHM = 172 nm. Standing Wave Microscopy (SWM), FWHM = 109 nm, Deconvolved. SWM, FWHM = 101 nm. All Images taken at Mag = 100x, NA = 1.45, 488 nm excitation, 100 nm Fluorescent Beads.

A SWM can improve the resolution in principle only by a factor of two, which was achieved when comparing WFM with SWM and comparing both deconvolved values. The AOD-based design increases flexibility and throughput of the SWM [3].

2.3 Frequency-Encoded Multi-Beam Microscope

Multi-point scanning will increase the imaging throughput if appropriate methods can be applied to separate simultaneous events. Telecom has perfected techniques for encoding and decoding signals to be sent over communication channels with limited bandwidth.
While random-access capability of AODs can be straightforwardly employed for time-multiplexing of multiple recording sites, another intrinsic property of AODs can be utilized for another encoding scheme, frequency multiplexing. The diffracted beam experiences a frequency shift caused by the acoustic wave (*Fig.7, Top*). Although the relative shift of the optical frequency is very small, $<10^{-6}$, and is ignored in most applications, it can be utilized for encoding purposes.

Frequency-encoding can be obtained by placing 2 AODs in the arms of an interferometer, causing an optical frequency shift in both beams equal to their individual acoustic waves. At the output of the interferometer, the amplitude will be modulated by the difference of both shifted optical frequencies, resulting in a beat frequency equal to the acoustic frequency difference (*Fig.7, Bottom*).

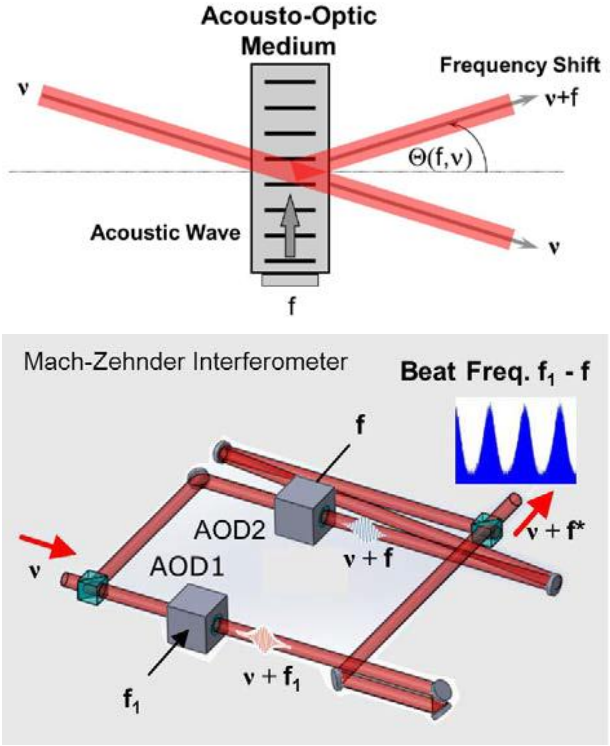

Figure 7. Frequency Shift of Optical Beam by AOD. *Top:* Shift of diffracted beam frequency (**ν + f**) by acoustic wave frequency **f**. *Bottom:* Beat frequency (**f1 - f**) at output of interferometer resulting from frequency shifts, **f, f1**, due to two independent AODs in each arm of the interferometer.

To utilize this for encoding during multi-site imaging, this effect needs to be extended to multiple beams. This is possible, since AODs can be used as adjustable multi-beam splitters. Simultaneously applied discrete acoustic frequencies result in a fan of multiple beams. The angle of each 1st order beam is proportional to the acoustic frequencies. Like in single beam deflection, frequency shifts are observed such that every individual beam becomes tagged with its acoustic frequency (*Fig.8*).

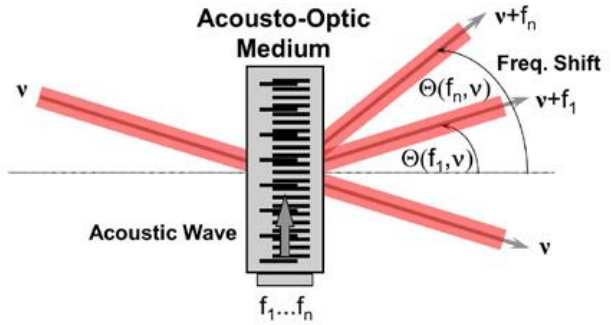

Figure 8. AOD as Multi-Beam Splitter and Multi-Frequency Shifter. Acoustic waves with multiple frequency components, $\mathbf{f_1 \ldots f_n}$, create complex diffraction patterns. Multiple beams with individual diffraction angles, $\mathbf{\Theta(f_1,\nu) \ldots \Theta(f_n,\nu)}$, and frequency shifts, $\mathbf{(\nu + f_1) \ldots (\nu + f_n)}$, are produced.

Applying the multi-frequency approach to our AOD-based Mach-Zehnder Interferometer results in a fan of beams at the output with individual beat frequencies (*Fig.9, Top*). To demonstrate the tagging effect, we applied three acoustic frequencies to the interferometer, simultaneously 85 MHz and 87 MHz to the AOD in one arm, and 80 MHz to the AOD in the other arm. The compound spectrum of both beams shows a typical amplitude-modulation (AM) pattern, with carrier and sidebands at the acoustic frequencies and the beat frequencies of 5 MHz and 7 MHz (*Fig.9, Bottom*).
To retrieve the encoded signals the compound fluorescence measurements, as seen by a single photodetector, have be decoded. This is traditionally done by bandpass filtering to separate the different beat frequencies. However, due to the stochastic nature of photons arriving at a detector, shot noise is detected along with the narrow-banded beat frequencies. This wide-band shot-noise causes unwanted crosstalk between recording sites.

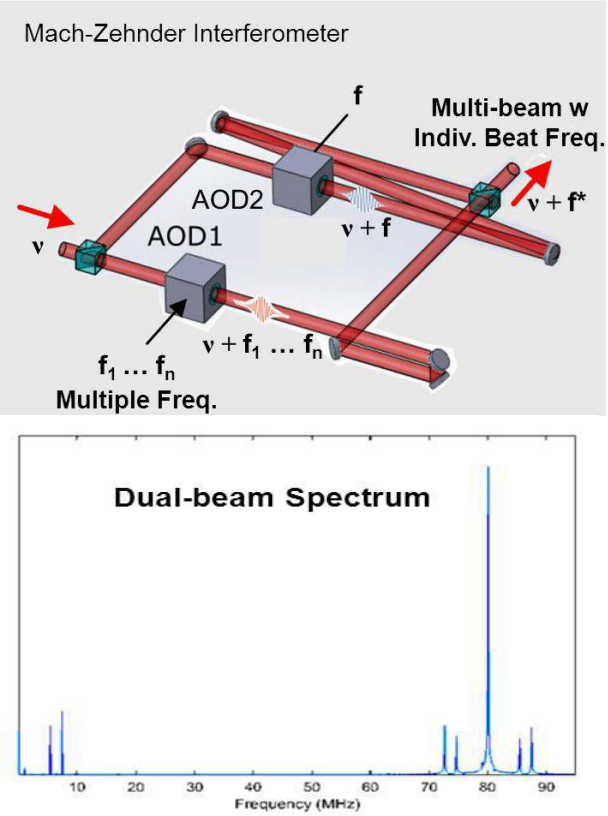

Figure 9. Frequency Encoding of Multiple Optical Beams by AODs. *Top:* Interferometer-generated multi-beams with beat frequencies, $\mathbf{(f_1 - f) \ldots (f_n - f)}$, resulting from different frequency shifts, $\mathbf{(\nu + f)_1 \ldots (\nu + f_n)}$, at two AODs. *Bottom:* Spectrum of two beams generated with AOD interferometer. Acoustic frequencies were 85 MHz and 87 MHz in AOD1, and 80 MHz in AOD2. Beat frequencies were 5 MHz and 7 MHz.

Sampling of the compound fluorescence at very high spatio-temporal resolution allows us to also determine the phase at each location of the sample. When averaging of samples within a certain bin is used without using the phase information, the decoded signals are crosstalk contaminated. Conversely, if phase-aligned averaging is applied, the crosstalk amongst signals is significantly reduced. Phase-aligned averaging uses time-shifting of measurements within a bin to avoid cancellation of modulated signal components (*Fig.10*).

This frequency-encoded microscope supports multi-beam imaging and largely avoids common crosstalk issues [5, 6].

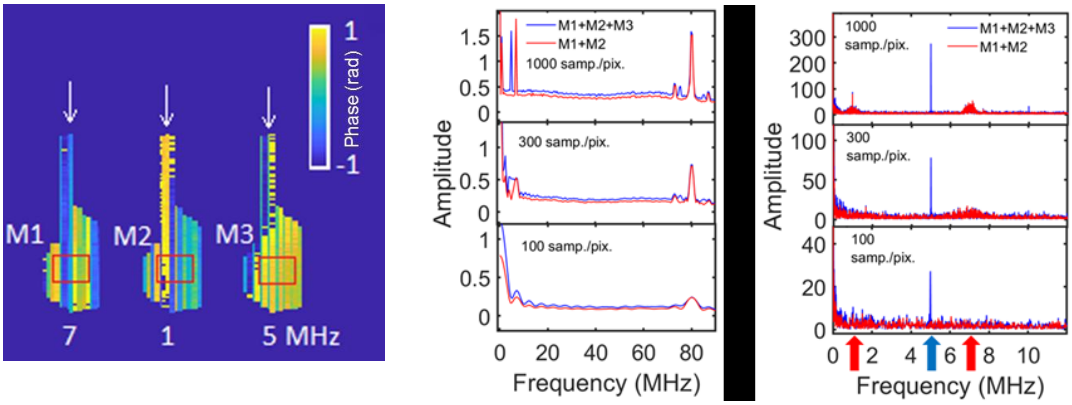

Figure 10. Phase-Aligned Averaging. *Left*: Single neuronal fluorescently labelled cell body scanned with three beams, encoded at 7 MHz, 1 MHz, and 5 MHz. Phase of detected fluorescence signal color-coded. Scan direction marked by arrows. *Middle*: Conventional average of samples within red bins M1 ... M3. *Right*: Same samples averaged after phase-aligning for 5 MHz encoding frequency. Note the significant reduction of channel crosstalk.

3. SUMMARY

Three types of acoustically controlled advanced light-microscopes were reviewed.

- **3D Random-Access Multi-Photon Microscope**: chirped acoustic waves in 4 sequential acousto-optic deflectors independently control collimation and angle of an ultra-fast laser beam to create a single focus positioned inertia-free in three dimensions.

- **Standing-Wave Super-Resolution Microscope**: position, separation, and phase of two diffraction-limited Fourier plane foci are controlled by acousto-optic deflectors to generate dynamic standing wave patterns with adjustable orientation, frequency, and phase.

- **Frequency-Encoded Multi-Beam Microscope**: a variable number of separate laser beams with individually controlled frequency-encoding are acousto-optically generated for simultaneous multi-site imaging.

4. AKNOWLEDGEMENTS

This work was supported by the US National Science Foundation, the US National Institutes of Health, the Allen Institute for Brain Science, Seattle WA, USA (AIBS), the Italian Institute of Technology, Genoa, Italy (IIT), and the University of Barcelona, Spain (UB).

List of major collaborators/contributors in alphabetical order: N. Ball (AIBS), P. Bianchini (IIT), J. Brockill (AIBS), W.E. Brownell (Baylor College of Medicine, Houston TX, USA), J.R. Cotton (BCM), A. Diaspro (IIT), M. Duocastella (IIT & UB), O. Gliko (BCM), V. Iyer (BCM), N. Orlova (AIBS), G.D. Reddy (BCM), A.S Tolias (BCM), D. Tsyboulski (AIBS).

5. REFERENCES

[1] G.D. Reddy, K. Kelleher, R. Fink, and P. Saggau. "Three-dimensional random access multiphoton microscopy for functional imaging of neuronal activity," *Nature Neuroscience,* vol. 11, no. 6, pp. 713-720, 2008.

[2] P. Saggau (Houston, TX), D. Reddy (Houston, TX), V. Iyer (Huntington, NY), "Method for high-speed microscopy with three-dimensional laser beam scanning," *US Patent* 7,332,705, 2008.

[3] O. Gliko, W.E. Brownell, P. Saggau, "Fast two-dimensional standing-wave total-internal-reflection fluorescence microscopy using acousto-optic deflectors," *Optics Letters*, vol. 34, no. 6, pp. 836-838, 2009.

[4] P. Bianchini (Genoa, IT), P. Saggau (Houston, TX), A. Diaspro (Genoa, IT). "Random access stimulated emission depletion (STED) microscopy," *US Patent* 9,810,966, 2017.

[5] D. Tsyboulski, N. Orlova, P. Saggau. "Amplitude modulation of femtosecond laser pulses in the megahertz range for frequency-multiplexed two-photon imaging," *Optics Express*, vol. 25, no. 8, pp. 9435, 2017.

[6] D. Tsyboulski, N. Orlova, P. Ledochowitsch, P. Saggau. "Two-photon frequency division multiplexing for functional in vivo imaging: a feasibility study," *Optics Express*, vol. 27, no. 4, pp. 4488, 2019.